Environment and Ecology 42 (3B) : 1332—1341, July—September 2024
Article DOI: https://doi.org/10.60151/envec/CYFV6307
ISSN 0970-0420

Synthesis, Characterization, and Process Optimization of Invasive Weed *Tephrosia purpurea* Biochar

Loveena Gaur, Poonam Poonia

Received 20 January 2024, Accepted 4 July 2024, Published on 4 September 2024

ABSTRACT

The present study aimed to optimize the pyrolysis process for producing biochar from the invasive weed *Tephrosia purpurea* using response surface methodology. The physico-chemical and morphological properties of biochar were predicted. The biochar was derived by slow pyrolysis at 450°C in vacuum conditions for 1 h of reaction time. The obtained biochar is rich in ketones, ethers, and aromatic compounds. Biochar has an alkaline pH, a high fixed carbon content (77.63%), a large surface area (87.77m^2/g), a wide pore volume (0.03724cm^3/g), and abundant trace minerals such as Na, K, Ca. Thus, findings reveal that obtained biochar could not only mitigate climate change, global warming, and carbon sequestration but also provide an effective strategy for invasive weed waste bio-management. To the best of the author's knowledge, the present study is the first to assess the potentiality of *T. purpurea* biochar obtained by slow and vacuum pyrolysis.

Keywords *Tephrosia purpurea,* Biochar, Vacuum pyrolysis, Optimization.

INTRODUCTION

Biomass energy is kinds of the alternative energy generated from renewable resources and are found abundantly. Biomass can be generally grouped into two categories, lignocellulosic and non-lignocellulosic biomass. The ligno-cellulosic biomass mainly includes agricultural residues, algal biomass, forest residues, manures, and energy crops (Moghtaderi *et al.* 2004). Non-lignocellulosic biomass used are sewage sludge, manure, algae, animal hair, feather, bone (Li and Jiang 2017). The chemical makeup of biomass varies based on the species and type of biomass, the growing conditions, and the geographical climate (Kan *et al*. 2016).

Biochar is a carbon-rich material created through the thermal decomposition of biomass at temperatures ranging from 300-900°C under oxygen-limited or oxygen -free conditions (Pandey *et al.* 2015). Biochar can be produced from biomass by different physical, thermochemical, and biochemical processes (Lehmann *et al.* 2011). The main thermochemical processes include gasification, pyrolysis, hydrothermal carbonization, and torrefaction. Among these, pyrolysis converts biomass into energy and chemical

Loveena Gaur[1], Poonam Poonia[2]*

[2]Assistant Professor
[1,2]Department of Zoology, Faculty of Science, Jai Narain Vyas University, Jodhpur 342011, Rajasthan, India

Email: poonam.poonia@yahoo.com
*Corresponding author

products such as solid (biochar), liquid (bio-oil), and gas (Wang and Wang 2019). The pyrolysis process can be categorized into slow and fast pyrolysis, depending on the temperature, heating rate, and residence time. The yield of biochar mainly depends on the type of pyrolysis. The biochar yield through slow pyrolysis is 30% and that through fast pyrolysis is 10-12% (Lee *et al.* 2013). Thus, for a high yield of biochar slow pyrolysis is most appropriate.

In recent years, biochar derived from invasive weed has attracted massive attention due to its potential effects (Ghosh and Maiti 2022). The invasive weed *Tephrosia purpurea* is a perennial legume shrub of the family Fabaceae that grows up to a height of 40–80 cm. It is a common wasteland weed with pantropical distribution. It originated from the Indian subcontinent and China and is found widespread all over the tropics. It can be found growing naturally on grassy fields, thickets, ridges, wastelands, and along roadsides (Orwa *et al*. 2009). One of the species of *Tephrosia* has been reported to contain 32.10% cellulose, 4.20% hemicelluloses, and 4.70 % lignin (Odedire and Babayemi 2008). In India, it is commonly known as purple bush bean, Indian hyacinth bean, Sarphonk, or Sharpunkha. Such biomass with less or no economic and medicinal value can be efficiently used in bioenergy production by thermodegradation. The main objective of this research is to analyze the utility of invasive weed *T. purpurea* biomass for biochar production through slow and vacuum pyrolysis at a temperature of 450°C. The characterization of biochar, such as proximate analysis (moisture content, ash content, fixed carbon, volatile content), elemental analysis (C, H, N, S), Brunauer –Emmet–Teller method (BET), Scanning electron microscopy (SEM), X-ray energy dispersive spectrometry (EDX), and Fourier transform infrared spectroscopy (FTIR), is presented to evaluate the physical, chemical, and morphological properties of biochar, so that its usability could be predicted and examined for sustainable environmental management.

MATERIALS AND METHODS

Biomass collection and biochar production: *T. purpurea* was collected from Jai Narain Vyas University, New Campus, Jodhpur, Rajasthan. The biomass samples were washed with water to remove soil particles and other debris. The samples were then placed in an open clean area under the sun for 10 days for solar drying. Biomass was chopped to attain uniform size of 50-100 mm. The dried samples were then subjected to vacuum pyrolysis at a temperature of 450°C with residence time of 60 min and a reduced pressure of 10–12 kPa to obtain carbon-rich material biochar.

The vacuum pyrolyzer consisted of a biomass cartridge, pyrolysis chamber, vacuum pump, electric heaters, insulation, shell- and tube -type condensers, and vacuum pump. The biomass is initially filled into the biomass cartridge, which is then inserted into the pyrolysis chamber. The pyrolysis chamber is connected to shell- and tube-type condensers and vacuum pump. To achieve the desired temperature for pyrolysis, electric coils are rolled over the pyrolysis chamber (Pawar and Panwar 2022). Gases and vapors produced during pyrolysis were passed away from the pyrolysis chamber using a vacuum pump. Shell- and tube -type condensers trapped the gasses produced and converted them into liquid oil, i.e., bio-oil. The obtained biochar was allowed to cool down at room temperature and then packed into air-tight polybags to avoid oxidation of the char.

Characterization of the biomass and biochar, pH and yield of biochar: Biochar pH was measured in 1:5, 1:10, and 1:20 biochar: Water (deionized water; DIW) ratios after 1 h of shaking. After this, samples were allowed to stand for 30 min and pH was measured (Lee *et al.* 2013). The yield of the biochar was calculated using the following formula given by Sadaka *et al.* (2014).

$$\text{Biochar yield (\%)} = \frac{\text{Weight of biochar (g)}}{\text{Weight of biomass (g)}} \times 100$$

Proximate and elemental analysis of biomass and biochar: The biomass and biochar were subjected to proximate analysis including moisture content, volatile content, fixed carbon content, and ash content (ASTM 3173–87 method). The presence of elements such as carbon, nitrogen, hydrogen, and sulfur in biomass and biochar were examined at the Central Salt and Marine Chemical Research Institute (CSMCRI), Bhavnagar, Gujarat, India, using an elemental ana-

lyzer (vario MICRO Cube). Oxygen was calculated using formula 1.

O% = 100 (%) - C (%) - H (%) - N (%) - Ash (%)
Formula 1

BET, SEM-EDX, and FTIR analysis of the biochar: The BET analysis of biochar was conducted at 197°C using the nitrogen sorption–desorption method to determine the total surface area, pore volume, and porosity (Micromeriti ASAP 2010). The surface morphology and localized elemental compositions (such as C, O, Na, Mg, K) of the biochar were examined using high-resolution scanning electron microscopy (SEM) and energy-dispersive X-ray spectroscopy (EDX) with a JEOL JSM 7100F. The FTIR analysis of biochar was carried out on an FTIR spectrometer (Cary 630 agilent technologies) at the Department of Chemistry, New Campus, Jai Narain Vyas University, Jodhpur, Rajasthan, India. The infrared spectrum of the powdered biochar sample was analyzed at room temperature with a resolution of 8.0 cm^{-1}, over a wavelength range of 650 cm^{-1} to 4000 cm^{-1}.

TGA analysis of the biomass: The dry weedy biomass was analyzed by thermogravimetric analysis (TGA) to determine the mass loss with increase in carbonized temperature. TGA of the feedstock was performed using a TG analyzer STA 7300. In the analysis, the powdered biomass was weighed (1–10 mg) and heated from normal to 900°C in the presence of a carrier gas, nitrogen, by maintaining a flow rate of about ml/min. Analysis was conducted at heating rates of 20°C/min.

Response surface methodology (RSM): Response surface methodology (RSM) was utilized to optimize the operating parameters of the vacuum pyrolytic unit for the production of high-quality biochar with a high yield. Operating parameters, such as biomass particle sizes, were varied within different ranges: less than 50 mm, between 50 and 100 mm, and greater than 100 mm, and were subsequently coded as -1, 0, and 1, respectively. Temperatures were varied between 350°C to 550°C. A central composite design (CCD) was employed to examine the effects of five independent variables on biochar properties: Carbon content, fixed carbon content, surface area, pore size, and pore volume. A total of 13 experimental runs were conducted based on the surface response of the CCD. Statistical and graphical analysis of the data were performed using Design Expert 13.0 software.

Table 1. pH of the various biochar.

Biomass	Pyrolysis temperature	Residence time	pH	Reference
T.purpurea	450 °C	60 min	9.6	Present study
Wood stem	500 °C	-	9.5	Haydary (2018)
Wood bark	500 °C	-	9.6	Haydary (2018)

RESULTS AND DISCUSSION

pH and yield of the biochar: The measured pH of *T. purpurea* was 9.6 (Table 1). Typically, the pH of biochar is alkaline, falling within the range of 7.1 to 10.5 (Lehmann *et al.* 2011). pH is greatly influenced by the pyrolysis temperature and contents of feedstock such as hemicellulose, cellulose, and lignin (Ronsse *et al*. 2012). Biochar functional groups such as –COO– and –O–and the carbonate content are attributed to its alkaline properties (Yuan *et al.* 2011). Similar observations for biochar alkalinity were reported by Haydary (2018) for wood bark and wood stem. A high yield of 30.18% biochar was obtained. The high yield of biochar is credited to a combination of factors, including slow pyrolysis under vacuum conditions and the utilization of lignocellulosic feedstock rich in inorganic elements (Tomczyk *et al.* 2020).

Proximate and elemental analysis of biomass and biochar: The proximate and elemental analysis of biomass and biochar from *T. purpurea* is outlined in Table 2. The pyrolysis temperature plays a significant role in altering properties such as volatile content, fixed carbon content, and ash content. Higher temperatures lead to a reduction in moisture and volatile content, accompanied by an increase in fixed carbon and ash content. In the present study, the moisture and volatile content decreased by 65.84% and 83.41%, respectively, while the fixed carbon content and ash content increased by 314.46% and 120.5% in biochar. Increase in temperature releases the volatile matter resulting into decreased volatile content as further cracking of volatile content produces low molecular weight liquids and gases (Yu *et al*. 2019). It is very

Table 2. Proximate and elemental composition of biochar and biomass of *T. purpurea.*

Proximate Analysis	Biomass (%)	Biochar (%)
Moisture content	6.91	2.36
Volatile content	70.06	11.62
Fixed carbon	18.73	77.63
Ash content	4.30	8.40
Elemental analysis		
Carbon	39.94	69.79
Nitrogen	1.78	1.90
Hydrogen	9.215	5.281
Sulfur	0.023	0.047
Oxygen	44.855	14.629
O/C	1.12	0.20
H/C	0.23	0.07
N/C	0.044	0.02

important to determine the elemental composition of biochar such as carbon, nitrogen oxygen, hydrogen and sulfur as they determine the properties and applicability of biochar. Carbon content in biochar increased by 74.73% whereas; hydrogen and oxygen content decreased by 42.69% and 67.38%. The lower is the molar ratios of O/C and H/C, the higher will be the elemental carbon. There occurs loss of oxygen and hydrogen during the pyrolysis process (Mary *et al.* 2016). Biochar with an H/C ratio less than 0.7 indicates a high level of aromaticity. (IBI 2015) and O/C between 0.2 and 0.6 shows moderate stability with half-life between 100 and 1000 years (Spokas 2010). The present study reported H/C and O/C ratio of biochar as 0.07 and 0.20 respectively. Therefore, the biochar obtained in this process aligns well with the standard parameters for high-quality biochar, exhibiting greater aromaticity, carbonization, and

Table 3. Percentage of localized carbon, oxygen and some minerals content by SEM-EDX analysis of the biochar (Weight % and atomic %).

Sl. No.	Element	Weight (%)	Atomic (%)
1	Carbon (C)	88.96	93.04
2	Oxygen (O)	6.97	5.47
3	Sodium (Na)	0.29	0.16
4	Magnesium (Mg)	0.55	0.28
5	Chloride (Cl)	0.42	0.15
6	Potassium (K)	2.23	0.72
7	Calcium (Ca)	0.57	0.18

enhanced stability in the environment.

BET and SEM-EDX analysis of biochar: *T. purpurea* biochar was found with large surface area, wide pore volume and small pore size of 87.77m^2/g, 0.03724 cm^3/g and 9.4733 nm respectively. The rise in pyrolysis temperature also correlates with an increase in the surface area and porosity of the biochar. This phenomenon is ascribed to the decomposition of organic matter and the subsequent formation of micropores (Bonelli *et al.* 2007). Reports indicate that heightened temperatures lead to the degradation of aliphatic alkyls, ester groups, and the aromatic lignin core, consequently resulting in an increase in surface area (Chen and Chen 2009). The micrographs of the biochar clearly depict well-developed pores on its surface (Fig. 1). Pores are orderly placed forming a system of well-developed pore structure. Pores are created due to volatilization of organic compounds during pyrolysis process. SEM/EDX analysis indicates the presence of carbon (88.96%) and oxygen (6.97%) as the major elements, along with trace minerals such as Na (0.29%), Mg (0.55%), K

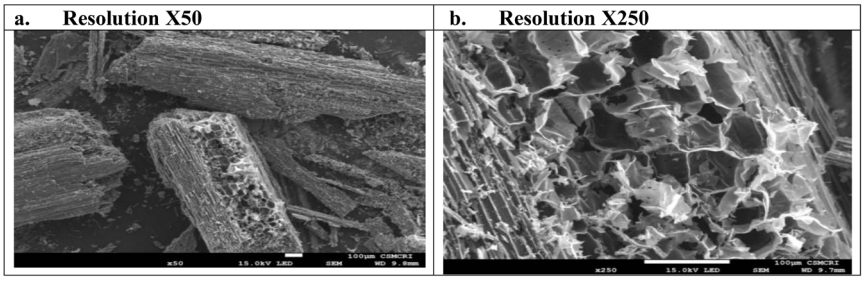

Fig. 1. Micrographs of pore structure of *T. purpurea* biochar obtained at 450 °C.

(2.23%) and Ca (0.57%) in biochar (Table 3). These are considered an important characteristic for soil amendment, since they are nutrient elements for plant growth (Rivka *et al.* 2017). Increased C-content indicates highest carbonization degree of biochar. A decrease in oxygen content signifies an increase in the surface hydrophobicity of the biochar, which is a significant factor in the removal of contaminants from aqueous matrices (Tomczyk *et al.* 2020).

Thermal characteristics of biomass: DTG curve gives the better indication of thermal decomposition of biomass components (Hemicellulose, cellulose, and lignin) (Rout *et al.* 2016). The mass loss curves of weed biomass for pyrolysis are presented in Fig. 2. The thermal decomposition mainly occurred in three stages, the first stage indicates the drying stage in which degradation occurred between 30-170°C in which 8% mass loss was observed. This stage is referred as passive zone due to hygroscopic nature of biomass (Said *et al.* 2013). The second stage is the devolatilization stage which is occurred in range of 170-380°C. In this stage maximum weight loss of 84% was observed. It is the most active stage of pyrolysis. Some non-condensable gases (CO, CO_2) and tarry gases containing organic compounds and carbon molecules are released (Nturanabo *et al.* 2010). In this stage, the temperature between 170-300°C denotes hemicellulose degradation whereas temperature 300-380°C shows cellulose degradation. A strong peak at 320°C between 200-400°C is attributed to pyrolysis of cellulose and hemicellulose (Yang *et al.* 2007). Degradation of lignin starts from 380°C showing broader peak and end into carbonization process at 560°C. Lignin is considered to be the hardest component of woody biomass for pyrolysis (Sahoo *et al.* 2021). The zone after 380°C is referred to as passive zone in which mass loss observed was low i.e. 3%. After 600°C the devolatilization process became almost stable, thus indicating pyrolysis completion (Pawar and Panwar 2022). The final by-products obtained are char and ash. It has been reported that hemicellulose and cellulose decomposition takes place at temperature range of 150–350°C and 275–350°C, and lignin decomposes very slowly till 900°C. Based on the TGA and DTG results, it was determined that the suitable temperature range for the pyrolysis zone is between 200°C and 600°C.

FTIR analysis of biochar: The FTIR spectrum of *T. purpurea* biochar is represented in Fig. 3. A very weak absorption peak at 3630 cm^{-1} between 3500-3900 cm^{-1} was observed representing –OH stretching vibration. It is characteristic of all cellulosic components (Schwanninger *et al.* 2004). Relatively weak peak attributes to loss of moisture due to high temperature during pyrolysis (Kim *et al.* 2014). No clear peaks are observed at 3200 cm^{-1}-3000 cm^{-1} indicating -OH functional group and at 3100 cm^{-1}-3000 cm^{-1} representing –CH functional group. This indicates the degradation of hemicellulose and cellulose at the specified pyrolytic temperature (Jouiad *et al.* 2015). A slight bending at 2363 cm^{-1} in 2500-2000 cm^{-1} range indicates that CO_2 was not fully removed from the background of air (Schott *et al.* 2021). The peaks observed at 1798 cm^{-1} and 1561 cm^{-1} in the range 2000 cm^{-1} -1500 cm^{-1} represents C=O stretching of aldehydes and ketones. It is formed due to the degradation of cellulose and hemicellulose, along with the in-plane C=C aromatic vibrations of skeletal compounds in lignin and extractives, respectively (Jouiad *et al.* 2015). This region is the most important region for carbonyl absorption.

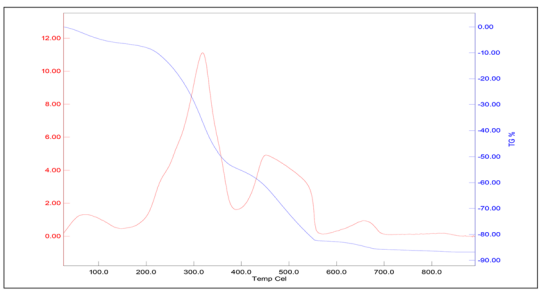

Fig. 2. TG and DTG curves of biochar of *T. purpurea.*

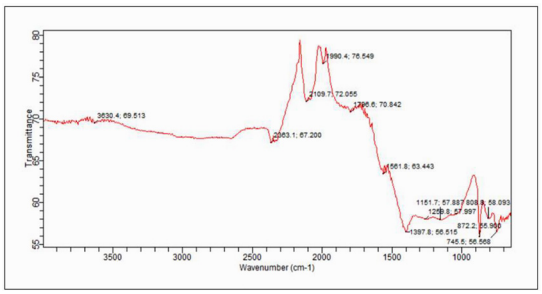

Fig. 3. FTIR spectral bands of *T. purpurea* biochar.

Peaks between range of 1400 cm^{-1}-900 cm^{-1} represents C=C rings of lignin. The emergence of peaks at 1397 cm^{-1}, 1259 cm^{-1}, and 1151 cm^{-1} could be attributed to symmetrical and asymmetrical aryl alkyl ethers. These peaks indicate changes in vibration due to the transformation products of the cellulose and lignin components of the biomass. These peaks are more pronounced than those for cellulose and hemicellulose which can be credited to lignin degradation temperature between 200-700°C (Jouiad *et al.* 2015). In the range between 900 cm^{-1} -700 cm^{-1} peaks are obtained at 872 cm^{-1}, 808 cm^{-1}, 745 cm^{-1} representing aromatic C-H bending vibration of benzene rings (Xu *et al.* 2013). From this, we can conclude that pyrolysis at 450°C leads to the degradation of cellulose and hemicellulose, while some aromatics related to lignin remain in the biochar.

Statistical significance of RSM results of *Tephrosia purpurea:* Table 4 presents the ANOVA results for the responses of carbon content, fixed carbon, surface area, pore size, and pore volume as obtained from the RSM study conducted using Design Expert 13.0. The F value and p-value for each model term were analyzed to identify the significance. The model F value for the responses of fixed carbon, carbon content, surface area, pore volume, and pore size were found to be 16.75, 383.32, 527.00, 182.41, and 75.14, respectively. These values indicate that the model is significant, with only a 0.09%, 0.01%, 0.01%, 0.01%, and 0.01% chance, respectively, that an F-value of this magnitude could occur due to noise. In this case, A, B, AB, AB^2 are significant model terms (A: Temperature, B: Particle size). For all the responses, p-value reported as less than 0.0500 indicate that the model terms are significant. Thus, confirming the

Table 4. ANOVA for the quadratic model based on the RSM design for various responses of *T. purpurea*.

Response	Source	Sum of squares	Df	Mean square	F value	p value	
Fixed carbon	**Model**	0.0357	5	0.0071	16.75	0.0009	Significant
	A-Temperature	0.0099	1	0.0099	23.21	0.0019	
	B-Particle size	0.0002	1	0.0002	0.3533	0.5709	
	AB	0.0021	1	0.0021	4.97	0.0610	
	A^2	0.0166	1	0.0166	38.85	0.0004	
	B^2	0.0008	1	0.0008	1.86	0.2147	
Carbon	**Model**	0.0516	5	0.0103	383.32	< 0.0001	Significant
	A-Temperature	0.0259	1	0.0259	962.23	< 0.0001	
	B-Particle size	0.0046	1	0.0046	171.53	< 0.0001	
	AB	0.0014	1	0.0014	52.40	0.0002	
	A^2	0.0174	1	0.0174	645.78	< 0.0001	
	B^2	0.0000	1	0.0000	1.38	0.2792	
Surface area	**Model**	0.0035	5	0.0007	527.00	< 0.0001	Significant
	A-Temperature	0.0007	1	0.0007	528.76	< 0.0001	
	B-Particle size	0.0004	1	0.0004	296.43	< 0.0001	
	AB	8.247E-06	1	8.247E-06	6.22	0.0413	
	A^2	0.0020	1	0.0020	1493.13	< 0.0001	
	B^2	3.270E-06	1	3.270E-06	2.47	0.1602	
Pore volume	**Model**	0.0000	5	7.377E-06	182.41	< 0.0001	Significant
	A-Temperature	0.0000	1	0.0000	275.65	< 0.0001	
	B-Particle size	7.196E-06	1	7.196E-06	177.94	< 0.0001	
	AB	7.751E-08	1	7.751E-08	1.92	0.2087	
	A^2	0.0000	1	0.0000	362.84	< 0.0001	
	B^2	1.160E-07	1	1.160E-07	2.87	0.1341	
Pore size	Model	0.0005	5	0.0001	75.14	< 0.0001	Significant
	A-Temperature	0.0001	1	0.0001	87.05	< 0.0001	
	B-Particle size	0.0002	1	0.0002	122.54	< 0.0001	
	AB	1.701E-10	1	1.701E-10	0.0001	0.9912	
	A^2	0.0002	1	0.0002	133.41	< 0.0001	
	B^2	1.022E-06	1	1.022E-06	0.7829	0.4056	

Table 5. Fit statistics of fixed carbon, carbon, surface area, pore volume and pore size.

Responses	Std. Dev.	Mean	CV%	R^2	Adjusted R^2	Predicted R^2	Adeq precision
Fixed carbon	0.0207	8.75	0.2360	0.9228	0.8677	0.3013	10.9071
Carbon	0.0052	9.00	0.0576	0.9964	0.9938	0.9652	62.2169
Surface area	0.0012	9.35	0.0123	0.9974	0.9955	0.9746	70.5712
Pore volume	0.0002	0.1909	0.1054	0.9924	0.9869	0.9639	43.8992
Pore size	0.0011	3.07	0.0372	0.9817	0.9686	0.9417	29.1498

hypothesis of the present study that particle size and temperature possess a significant effect on all the selected responses.

Furthermore, the statistical fitting analysis of responses for fixed carbon, carbon content, surface area, pore volume, and pore size reveal R^2 values of 0.9228, 0.9964, 0.9974, 0.9924, and 0.9817, respectively (Table 5). These values, which are close to 1, indicate a significant fit for the regression model. For carbon, the predicted R^2 of 0.9652 is in reasonable agreement with the adjusted R^2 of 0.9938, with a dif-

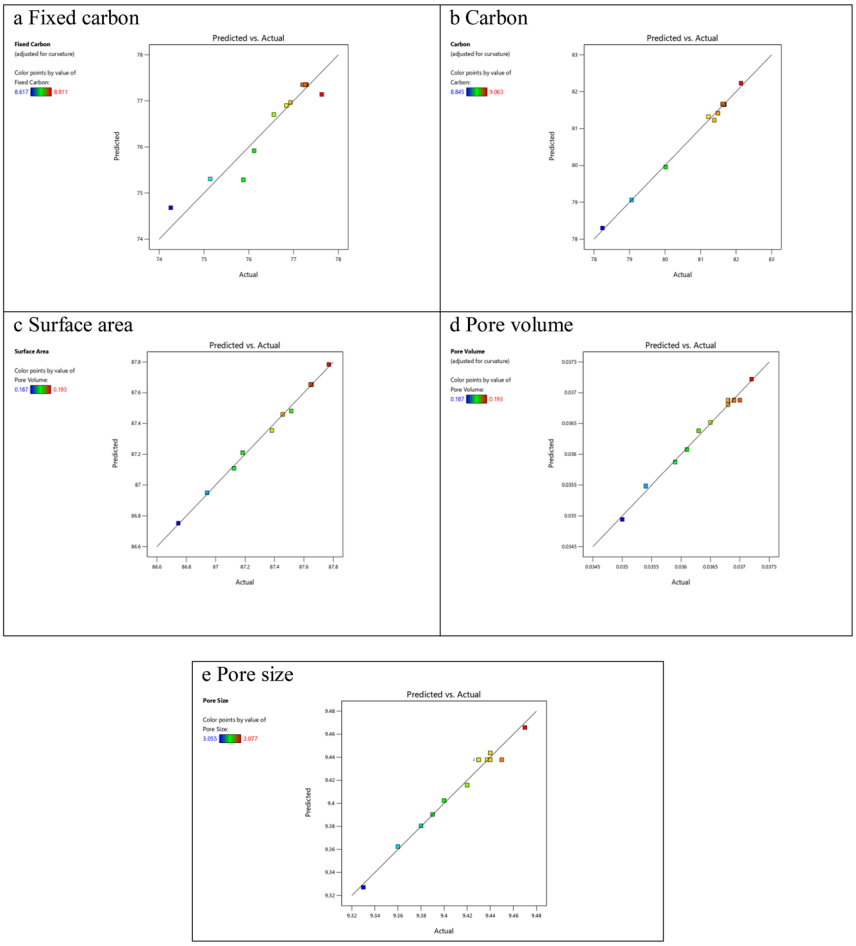

Fig. 4. Predicted vs actual plots of responses for *T. purpurea*.

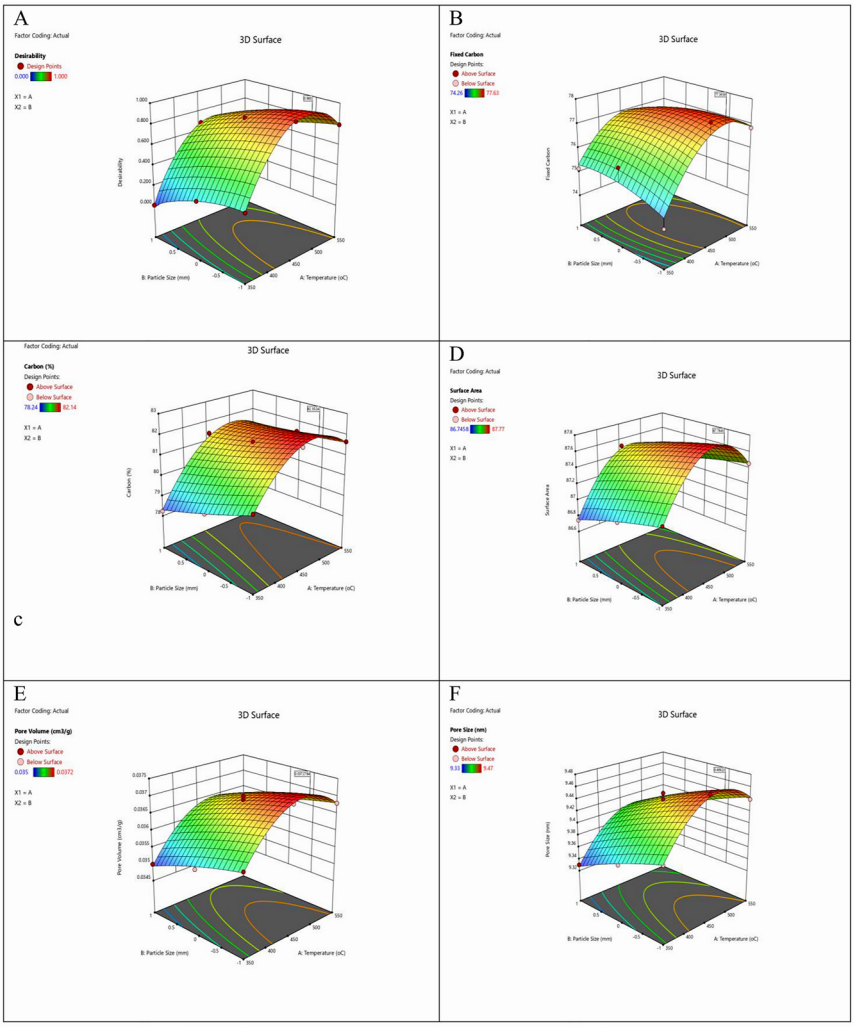

Fig. 5. Three-dimensional response surface plots (a, b, c, d, e, f) for desirability, fixed carbon, carbon, surface area, pore volume, and pore size of *T. purpurea.*

ference of less than 0.2. This indicates that the model can predict the response accurately. Similar results were observed for surface area, pore volume, and pore size, where the predicted R^2 values (0.9746, 0.9639, and 0.9417 respectively) were found to be in reasonable agreement with the adjusted R^2 values (0.9955, 0.9869, and 0.9686 respectively), with differences of less than 2. This suggests that the model is excellent in accurately predicting the response. Fit statistics for fixed carbon shows that the predicted R^2 of 0.3013 is not as close to the adjusted R^2 of 0.8677 with the difference more than 0.2. This may indicate a large block effect or a possible problem with used model and/or data. The Adeq Precision measures the signal-to-noise ratio. With values of 10.907, 62.217, 70.571, 43.899, and 29.150 for fixed carbon, carbon content, surface area, pore volume, and pore size respectively, the signal-to-noise ratios are deemed adequate as they exceed 4, which are considered desirable (Table 5). This suggests that the model can effectively navigate the design space. Additionally, the coefficient of variation (CV%) for all responses is observed to be

less than 10%, indicating a good model.

Figure 4. Illustrates the correlation between the predicted and actual values, showing strong linearity. This indicates that the employed model is useful for efficiently predicting fixed carbon, carbon content, surface area, pore volume, and pore size. The predicted values are closely clustered around the regression line, indicating good agreement between the predicted and actual values. This suggests that the predicted values for achieving good quality biochar align well with the actual results. Figure 5. exhibits three-dimensional RSM plots of the various components. The 3-D response surface depicts two independent variables on the x-axis (temperature) and y-axis (particle size), with the response presented on the z-axis. These plots illustrate the effects of temperature and particle size on various responses. The responses indicate increased attractiveness at particle sizes between 50 and 100 mm. The reactivity area decreases with increasing particle size, which may be associated with enhanced pyrolysis and higher ash conversion. At ideal temperatures, larger surface area and pore volume are preferable for effective adsorption. It is concluded that the optimum values for fixed carbon, carbon content, surface area, pore volume, and pore size may be achieved at 484.902°C, which aligns well with the outcomes observed at 450°C.

CONCLUSION

Biomass of invasive weeds *T. purpurea* proves to be potential precursor to biochar. The optimum operating condition for conversion of feedstock into quality biochar were predicted by response surface methodology with CCD as experimental design to maximize the responses surface area, carbon content, fixed carbon, pore size, and pore volume. This study reports that both pyrolysis temperature and feedstock particle size have a significant impact on the physico-chemical and morphological characteristics of biochar. In the present research work biochar was derived by slow and vacuum pyrolysis of feedstock of 50-100 mm at temperature 450°C for one hour of residence time. The results indicated that optimum preparation parameters have produced biochar of high yield 30.18% with amplified quality of all responses. The decreased O/C and H/C molar ratios indicate significant aromaticity and enhanced stability of the biochar in the environment. The findings of the study could reflect the potential usability of *T. purpurea* biochar for increased soil carbon; improve agricultural production, reduction/immobilization of environmental pollutants. Apart from this, reduction of hazardous invasive weed waste biomass to derive biochar could provide the possible way to solve the management and disposal of invasive weed in efficient, environment friendly and sustainable manner.

ACKNOWLEDGMENT

The authors are very thankful to Dr N. L. Panwar and Department of Renewable Energy Engineering, MPUAT, Udaipur, Rajasthan for providing the laboratory facilities and constant guidance during the research work.

REFERENCES

Bonelli PR, Buonomo EL, Cukiermanm AL (2007) Pyrolysis of sugarcane bagasse and co-pyrolysis with an argentinean subbituminous coal. *Energy Sources Part A* 29: 731–740. DOI: https://doi.org/10.1080/00908310500281247

Chen B, Chen Z (2009) Sorption of naphthalene and 1-naphthol by biochars of orange peels with different pyrolytic temperatures. *Chemosphere* 76: 127–133. DOI: https://doi.org/10.1016/j.chemosphere.2009.02.004

Ghosh D, Maiti SK (2022) Invasive weed-based biochar facilitated the restoration of coal mine degraded land by modulating the enzyme activity and carbon sequestration. *The Journal of the Society for Ecological Restoration* 31: 3. DOI: https://doi.org/10.1111/rec.13744

Haydary J (2018) Aspen simulation of two stage pyrolysis/gasification of carbon based solid waste. *Chemical Engineering Transactions* 70: 1033. DOI: https://doi.org/10.3303/CET1870173

International Biochar Initiative (IBI) (2015) Standardized Product Definition and Product Testing Guidelines for Biochar that Is Used in Soil. Version 2.1, 23 November (2015) (Document Reference Code: IBI-STD-2.1).

Jouiad M, Al-Nofeli N, Khalifa N, Benyettou F, Yousef LF (2015) Characteristics of slow pyrolysis biochars produced from Rhodes grass and frons of edible date palm. *Journal of Analytical and Applied Pyrolysis* 111: 183. DOI: https://doi.org/10.1016/j.jaap.2014.10.024

Kan T, Strezov V, Evans TJ (2016) Lignocellulosic biomass pyrolysis: A review of product properties and effects of pyrolysis parameters. *Renewable and Sustainable Energy Reviews* 57: 1126-1140. DOI: https://doi.org/10.1016/j.rser.2015.12.185

Kim P, Hensely D, Labbe N (2014) Nutrient release from switchgrass derived biochar pellets embedded with fertilizer. *Geoderma* 4:341-351. DOI: https://doi.org/10.1016/j.geoderma.2014.05.017

Lee Y, Park J, Ryu C, Gang KS, Yang W, Park YK, Jung J, Hyun S (2013) Comparison of biochar properties from biomass residues produced by slow pyrolysis at 500°C. *Bioresource Technology* 148:196–201. DOI: https://doi.org/ 10.1016/j.biortech.2013.08.135

Lehmann J, Rilig MC, Thies J, Masiello CA, Hockaday WC, Crowley D (2011) Biochar effects on soil biota—A review. *Soil Biology and Biochemistry* 43: 1812–1836. DOI: https://doi.org/10.1016/j.soilbio.2011.04.022

Li D, Jiang H (2017) The thermochemical conversion of non-lignocellulosic biomass to form biochar: A review on characterizations and mechanism elucidation. *Bioresource Technology* 246: 57-68. DOI: https://doi.org/10.1016/j.biortech.2017.07.029

Mary GS, Sugumaran P, Nivedhitha S, Ramalakshmi B, Ravichandran P, Seshadri S (2016) Production, characterization and evaluation of biochar from pod (*Pisum sativum)*, leaf (*Brassica oleracea*) and peel (*Citrus sinensis*) wastes. *International Journal of Recycling Organic Waste in Agriculture* 5:43. DOI: https://doi.org/10.1007/s40093-016-0116-8

Moghtaderi B, Meesri C, Wall TF (2004) Pyrolytic characteristics of blended coal and woody biomass. *Fuel* 83(6):745-750. DOI: https://doi.org/10.1016/j.fuel.2003.05.003

Nturanabo F, Byamuisha G, Preti G (2010) Performance appraisal of the casamance kiln as replacement to the traditional kilns in Uganda. In: Second International Conference on Advances in Engineering and Technology.

Odedire JA, Babayemi OJ (2008) Comparative studies on the yield and chemical composition of *Panicum maximum* and *Andropogon gayanus* as influenced by *Tephrosia candida* and *Leucaena leucocephala*. *Livestock Research for Rural Development* 20 (2): In prees.

Orwa C, Mutua A, Kindt R, Jamnadass R, Anthony S (2009) Agroforestree database; a tree reference and selection guide version 4.0", World Agroforestry Center, Kenya.

Pandey A, Bhaskar T, Stocker M, Sukumaran R (2015) Recent Advances in Thermochemical Conversion of Biomass. Elsevier, Amsterdam, Netherlands, pp 3-30.

Pawar A, Panwar NL (2022) A comparative study on morphology, composition, kinetics, thermal behavior and thermodynamic parameters of *Prosopis juliflora* and its biochar derived from vacuum pyrolysis. *Bioresource Technology Reports* 18:101053. DOI: https://doi.org/10.1016/j.biteb.2022.101053.

Rivka B, Laird D, Thompson M, Lawrinenko M (2017) Characterization and quantification of biochar alkalinity. *Chemosphere* 167:367-373. DOI: 10.1016/j.chemosphere.2016.09.151.

Ronsse F, Van Hecke S, Dickinson D, Prins W (2012) Production and characterization of slow pyrolysis biochar: Influence of feedstock type and pyrolysis conditions. *Global Change Biology Bioenergy* 5:104–115. DOI: https://doi.org/10.1111/gcbb.12018.

Rout T, Pradhan D, Singh RK, Kumari N (2016) Exhaustive study of products obtained from coconut shell pyrolysis. *Journal of Environmental Chemical Engineering* 4 (3): 3696–3705. DOI:https://doi.org/10.1016/j.jece.2016.02.024

Sadaka S, Sharara MA, Ashworth AJ, Keyser P, Allen F, Wright A (2014) Characterization of biochar from switchgrass carbonization. *Energies* 7(2): 548- 567. DOI: 10.3390/en7020548

Sahoo SS, Vijay VK, Chandra R, Kumar H (2021) Production and characterization of biochar produced from slow pyrolysis of pigeon pea stalk and bamboo. *Cleaner Engineering and Technology* 3: 100101. DOI: https://doi.org/10.1016/j.clet.2021.100101

Said N, Bishara T, Garcia-Maraver A, Zamorano M (2013) Effect of water washing on the therma behavior of rice straw. *Waste Management* 33(11): 2250-2256. DOI: https://doi.org/10.1016/j.wasman.2013.07.019

Schott JA, Do-Thanh CL, Shan W, Puskar NG, Da S, Mahurin SM (2021) FTIR investigation of the interfacial properties and mechanisms of CO_2 sorption in porous ionic liquids. *Green Chemical Engineering* 2 (4): 392-401. DOI: https://doi.org/10.1016/j.gce.2021.09.003

Schwanninger M, Rodrigues JC, Pereira H, Hinterstoisser B (2004) Effects of short-time vibratory ball milling on the shape of FTIR spectra of wood and cellulose. *Vibrational Spectroscopy* 36(1): 23–40. DOI: https://doi.org/10.1016/j.vibspec.2004.02.003

Spokas KA (2010) Review of the stability of biochar in soils: Predictability of O:C molar ratios. *Carbon Management* 1(2): 289–303. DOI: https://doi.org/10.4155/cmt.10.32

Tomczyk A, Sokołowska Z, Boguta P (2020) Biochar physicochemical properties: Pyrolysis temperature and feedstock kind effects. *Reviews in Environmental Science and Biotechnology* 19:191–215. DOI:10.1007/s11157-020-09523-3

Wang J, Wang S (2019) Preparation, modification and environmental application of biochar: A review. *Journal of Cleaner Productions* 227: 1002-1022. DOI: https://doi.org/10.1016/j.jclepro.2019.04.282

Xu X, Cao X, Zhao L (2013) Comparison of rice husk and dairy manure- derived biochars for simultaneously removing heavy metals from aqeous solution: Role of mineral components in biochar.*Chemosphere* 92: 955-961. DOI: https://doi.org/10.1016/j.chemosphere.2013.03.009

Yang H, Yan R, Chen H, Lee DH, Zheng C (2007) Characteristics of hemicellulose, cellulose and lignin pyrolysis. *Fuel* 86: 1781–1788. DOI: 10.1016/j.fuel.2006.12.013.

Yuan JH, Xu RK, Zhang H (2011) The forms of alkali in biochar produced from crop residues at different temperatures. *Bioresource Technology* 102: 3488-3497. DOI: https://doi.org/10.1016/j.biortech.2010.11.018

Yu S, Park J, Kim M, Ryu C, Park J (2019) CO_2 absorption by cryogels produced from poultry litter wastes. Bioresource Technology Reports, pp 6- 217. DOI: https://doi.org/10.1590/0104-1428.210075